Acoustic and photoacoustic microscopy of single leukocytes

Eric M. Strohm, Michael J. Moore, Michael C. Kolios*

Department of Physics, Ryerson University, Toronto, Canada
Institute for Biomedical Engineering, Science and Technology (iBEST), a partnership between Ryerson University and St. Michael's Hospital, Toronto, Canada
Keenan Research Centre for Biomedical Science of St. Michael's Hospital, Toronto, Canada
*mkolios@ryerson.ca

ABSTRACT

An acoustic/photoacoustic microscope was used to create micrometer resolution images of stained cells from a blood smear. Pulse echo ultrasound images were made using a 1000 MHz transducer with 1 μm resolution. Photoacoustic images were made using a fiber coupled 532 nm laser, where energy losses through stimulated Raman scattering enabled output wavelengths from 532 nm to 620 nm. The laser was focused onto the sample using a 20x objective, and the laser spot co-aligned with the 1000 MHz transducer opposite the laser. The blood smear was stained with Wright-Giemsa, a common metachromatic dye that differentially stains the cellular components for visual identification. A neutrophil, lymphocyte and a monocyte were imaged using acoustic and photoacoustic microscopy at two different wavelengths, 532 nm and 600 nm. Unique features in each imaging modality enabled identification of the different cell types. This imaging method provides a new way of imaging stained leukocytes, with applications towards identifying and differentiating cell types, and detecting disease at the single cell level.

Keywords: Acoustic microscopy, photoacoustic microscopy, blood smear

1. INTRODUCTION

Acoustic microscopy uses ultra-high frequency pulse-echo ultrasound to image single cells with micrometer resolution[1,2]. Depending on the imaging mode, the image contrast depends on the attenuation or scattering of the sound waves due to the biomechanical properties of the cell[3]. Photoacoustic microscopy (PAM) adds a laser to the ultrasound hardware, enabling the measurement of photoacoustic waves in addition to ultrasound pulse-echo waves. Through absorption of the laser energy, structures in the cell emit an acoustic wave which can be detected using the same transducer used in acoustic microscopy[4]. Different chromophores in the cell, including hemoglobin, melanin, and DNA, can be targeted by using different laser wavelengths or by using external stains to induce photoacoustic waves[5–7].

Optical-resolution photoacoustic microscopy (OR-PAM) provides resolution better than 1 μm by focusing the laser to a diffraction limited spot and detecting photoacoustic waves with ultrasound transducers in the 20-80 MHz range[8–10]. In ultrasound imaging, the ultrasound frequencies in this range have a lateral resolution over 20 μm, and thus are unsuitable for imaging single cells. Using transducers with frequencies in the 1000 MHz range enables pulse-echo ultrasound imaging with 1 μm resolution[11].

Combined ultrasound and photoacoustic imaging with 1 μm resolution was performed on a blood smear stained with Wright-Giemsa. This colorimetric Romanowksy dye stains the different types of organelles found in leukocytes different colors, enabling visual identification of the cell types as well as different pathological conditions that may be present[12]. Common leukocytes including a neutrophil, lymphocyte and a monocyte were imaged with ultrasound and photoacoustics at 532 nm and 600 nm and a 1000 MHz ultrasound transducer. Unique features in each cell type could be identified according to the unique ultrasound and photoacoustic images.

Photons Plus Ultrasound: Imaging and Sensing 2016, edited by Alexander A. Oraevsky, Lihong V. Wang
Proc. of SPIE Vol. 9708, 97082G · © 2016 SPIE · CCC code: 1605-7422/16/$18 · doi: 10.1117/12.2211759

2. METHOD

2.1 Sample preparation

A blood smear was prepared using a drop of blood extracted from a healthy volunteer in accordance with Ryerson University Ethics Review Board (REB #2012-210). The blood was allowed to dry, and then methanol was applied to fix the cells. One mL of Wright-Giemsa stain (Sigma Aldrich, USA) was applied directly to the slide for one minute, and then 1 mL of deionized water was added for 2 minutes. The slide was then washed with deionized water and left to dry before imaging.

2.2 Acoustic and photoacoustic measurements

All ultrasound and photoacoustic imaging was performed using an acoustic/photoacoustic microscope (Kibero GmbH, Germany). This system consists of an inverted optical microscope, an ultrasound transducer which records measurements from above the sample stage, and a 532 nm laser (Teem Photonics, France) is focused through the side port onto the sample from below using a 20x objective (figure 1). The optics and transducer were co-aligned, enabling ultrasound and photoacoustic measurements of the same area. Single cells were targeted using an optical view through a CCD (figure 2). The pulsed laser was fiber coupled; through cascaded stimulated Raman scattering within the fiber, energy losses enabled additional wavelengths from the fiber from 532-620 nm as shown in figure 2 [13,14]. The absorption spectrum of the Wright-Giemsa stain is shown in figure 2, measured using a UV-3600 spectrophotometer (Himadzu, Japan). Photoacoustic images were created at two wavelengths by using filters to select either 532 nm, or 600 nm. Laser energies from 1-5 nJ/pulse were used. Ultrasound images were measured first, followed by photoacoustic imaging at 532 nm and then at 600 nm. Scans were made using a 20x20 μm area with a 0.33 μm step size with 100 point signal averaging. Signals were amplified by 40 dB (Miteq, USA) and then digitized at 8 GS/s (Acqiris, USA). Further details on the acoustic and photoacoustic system and methods can be found in [15,16].

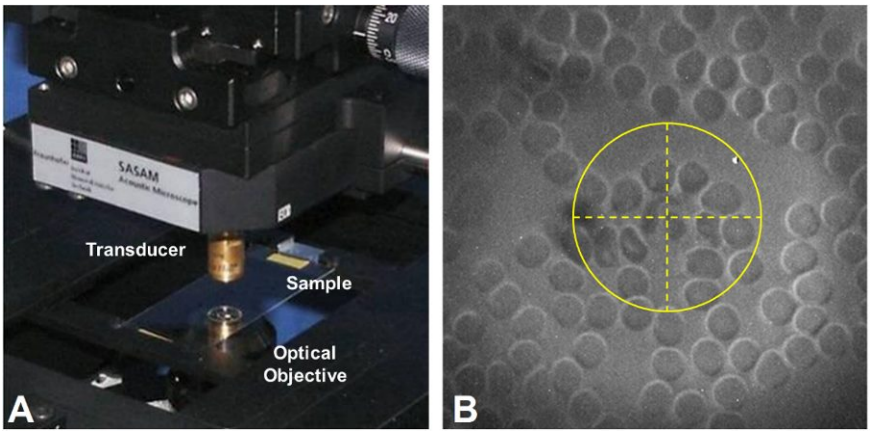

Figure 1: (A) The acoustic microscope. The slide to be measured is positioned between the transducer and microscope optics (image courtesy Robert Lemor, Kibero GmbH). (B) A live view of the sample before a measurement. The crosshairs are aligned to the ultrasound and photoacoustic focal spots, enabling targeting of single cells. A neutrophil surrounded by many red blood cells are visible within the crosshairs.

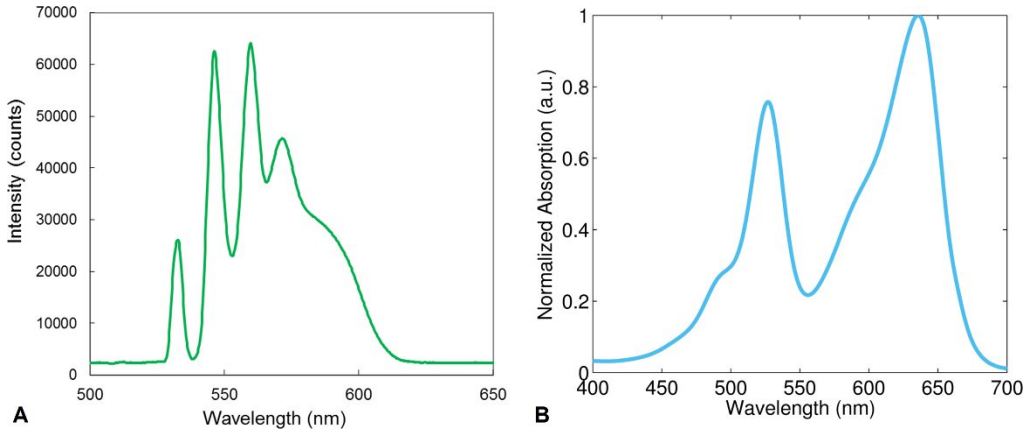

Figure 2: (A) The wavelengths from the fiber-coupled 532 nm laser. Energy loses due to stimulated Raman scattering increase the laser wavelengths beyond the nominal operating 532 nm output from the laser. (B) The absorption spectrum of the Wright-Giemsa stain.

3. RESULTS AND DISCUSSION

The optical, ultrasound and photoacoustic images of a neutrophil, lymphocyte and a monocyte, the most common leukocytes found in blood, are shown in figure 3. The optical images show the traditional staining profiles of the leukocytes. Neutrophils have a light pink cytoplasm and blue nuclei, lymphocytes have a light blue cytoplasm and a dark blue nucleus, and the monocytes have a light purple cytoplasm and dark purple nucleus. In addition to unique color staining, these leukocytes also have unique physical characteristics that can be used to help identification. Neutrophils tend to have multi-lobed nuclei with 3-5 lobes, lymphocytes have a large nuclei encompassing most of the cell, while monocytes tend to be larger with a kidney-bean shaped nucleus. In some cases however, these cells can be difficult to differentiate using conventional optical microscopy.

The acoustic images showed attenuation through different areas of the cells. In neutrophils, the strongest attenuation generally occurred through the nucleus, however attenuation was also observed through areas that did not coincide directly with the stained nucleus. In another study, an increase in the ultrasound attenuation was observed in the nuclei of stained neutrophils using transmission acoustic microscopy [17]. In contrast, the cytoplasm of the lymphocytes and monocytes were more attenuating than the nucleus, which is the opposite of what was observed with the neutrophils. For both the lymphocyte and monocyte, the acoustic image of the nucleus was clearly delineated, unlike with the neutrophil. It is possible that the stains increased the ultrasound attenuation at the 1000 MHz frequencies used.

The photoacoustic images provided the greatest contrast between cell types. A strong photoacoustic signal was measured from the neutrophil nuclei at both 532 nm and 600 nm, with negligible signals detected from the cytoplasm. In the lymphocytes, the photoacoustic signal from the nucleus was much stronger than the cytoplasm at 532 nm, however, this trend was reversed at 600 nm with a stronger signal detected from the cytoplasm than the nucleus. The monocytes showed a strong photoacoustic signal from the nucleus at both 532 nm and 600 nm. Although a stronger signal from the cytoplasm was measured at 600 nm than 532 nm, the signal from the nucleus was greater in both cases. A signal from the vacuoles present in the monocyte was very low, likely due to the lack of staining within this organelle. Additional features were observed in the photoacoustic images that were not easily discernible in the optical images. For example, in the lymphocyte, a bright region in the nucleus was observed, which coincides with the increased area of attenuation in the ultrasound image.

These results demonstrate that high resolution acoustic and photoacoustic imaging can be used to identify different leukocytes found in a stained blood smear. The photoacoustic images provide additional details and accentuate features that may not be present in conventional optical imaging. This is primarily due to the differential staining provided by the Wright-Giemsa stain, and the strong absorption of the stain constituents at the wavelengths used. Future work will focus on using more optical wavelengths, and examining blood smears exhibiting pathological features which may be easier to detect using acoustic and photoacoustic imaging compared to optical imaging alone.

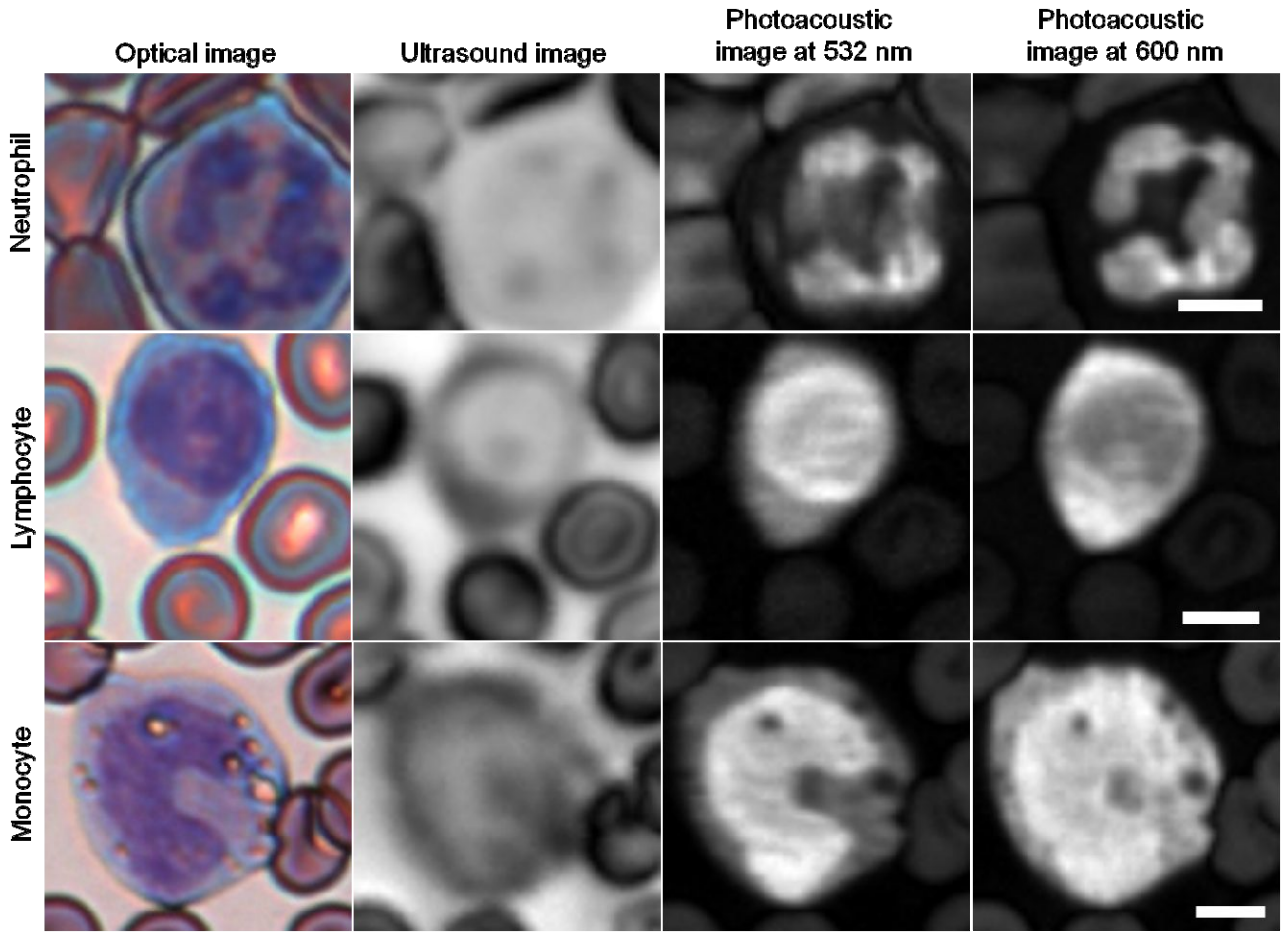

Figure 3: Optical, acoustic and photoacoustic images of a neutrophil (top), a lymphocyte (middle) and a monocyte (bottom) from a stained blood smear. The photoacoustic images were made using two wavelengths, 532 nm and 600 nm.The scale bar is 5 μm.

4. CONCLUSIONS

This study demonstrates the first combined acoustic and multispectral photoacoustic imaging of single cells at 1000 MHz. At this frequency, both the acoustic resolution and photoacoustic resolution is 1 μm, providing excellent lateral resolution in both imaging modalities. A neutrophil, lymphocyte and a monocyte from a stained blood smear were examined, and unique features acoustic and photoacoustic images could be used to identify the cell types. In the future, this combined imaging modality could be used to investigate pathological features in cells which would be difficult to detect using conventional microscopy methods alone.

5. ACKNOWLEDGEMENTS

This research was undertaken, in part, thanks to funding from The Canadian Cancer Society generously supported by the Lotte & John Hecht Memorial Foundation, the Natural Sciences and Engineering Research Council of Canada, and the Canada Research Chairs Program. Funding to purchase the equipment was provided by the Canada Foundation for Innovation, the Ontario Ministry of Research and Innovation, and Ryerson University.

REFERENCES

[1] Lemons, R.A., and Quate, C.F., "A Scanning Acoustic Microscope," in Proceedings of the IEEE Ultrasonics Symposium, 18– 21 (1973).

[2] Lemons, R.A., and Quate, C.F., "Acoustic microscope—scanning version," Applied Physics Letters 24(4), 163 (1974).

[3] Briggs, A., and Kolosov, O., [Acoustic microscopy], Oxford University Press, USA (2009).

[4] Xu, M., and Wang, L.V., "Photoacoustic imaging in biomedicine," Review of Scientific Instruments 77(4), 041101–041101–22 (2006).

[5] Rao, B., Maslov, K., Danielli, A., Chen, R., Shung, K.K., Zhou, Q., and Wang, L.V., "Real-time four-dimensional optical-resolution photoacoustic microscopy with Au-nanoparticle assisted sub-diffraction-limit resolution," Optics letters 36(7), 1137–1139 (2011).

[6] Danielli, A., Maslov, K., Garcia-Uribe, A., Winkler, A.M., Li, C., Wang, L., Chen, Y., Dorn, I. Gerald W., and Wang, L.V., "Label-free photoacoustic nanoscopy," Journal of Biomedical Optics 19(8), 086006–086006 (2014).

[7] Strohm, E.M., Moore, M.J., and Kolios, M.C., "Single cell photoacoustic microscopy: a review," IEEE Journal of Selected Topics in Quantum Electronics 22(3), (2016).

[8] Yao, J., and Wang, L.V., "Sensitivity of photoacoustic microscopy," Photoacoustics 2(2), 87–101 (2014).

[9] Yao, J., and Wang, L.V., "Photoacoustic microscopy," Laser & Photonics Reviews 7(5), 758–778 (2013).

[10] Wang, L.V., "Multiscale photoacoustic microscopy and computed tomography," Nature Photonics 3(9), 503–509 (2009).

[11] Strohm, E.M., Czarnota, G.J., and Kolios, M.C., "Quantitative measurements of apoptotic cell properties using acoustic microscopy," IEEE Transactions on Ultrasonics, Ferroelectrics and Frequency Control 57(10), 2293–2304 (2010).

[12] Horobin, R.W., and Walter, K.J., "Understanding Romanowsky staining. I: The Romanowsky-Giemsa effect in blood smears," Histochemistry 86(3), 331–336 (1987).

[13] Hajireza, P., Forbrich, A., and Zemp, R., "In-Vivo functional optical-resolution photoacoustic microscopy with stimulated Raman scattering fiber-laser source," Biomedical Optics Express 5(2), 539–546 (2014).

[14] Buma, T., Wilkinson, B.C., and Sheehan, T.C., "Near-infrared spectroscopic photoacoustic microscopy using a multi-color fiber laser source," Biomedical Optics Express 6(8), 2819 (2015).

[15] Strohm, E.M., Berndl, E.S.L., and Kolios, M.C., "High frequency label-free photoacoustic microscopy of single cells," Photoacoustics 1(3–4), 49–53 (2013).

[16] Strohm, E.M., Berndl, E.S.L., and Kolios, M.C., "Probing red blood cell morphology using high frequency photoacoustics," Biophysical Journal 105(1), 59–67 (2013).

[17] Lemons, R., and Quate, C., "Acoustic microscopy: biomedical applications," Science 188(4191), 905 –911 (1975).